Vertical Microstructure Measurements in the Central North Pacific

M. C. Gregg, C. S. Cox and P. W. Hacker[1]

Scripps Institution of Oceanography, University of California, San Diego 92037

(Manuscript received 13 March 1973, in revised form 9 May 1973)

ABSTRACT

Temperature profiles were made, during a period of calm weather in early autumn, in the center of the subtropical gyre in the North Pacific with free-fall microstructure instruments as well as with commerical salinity-temperature-depth recorders. In the depth range of 0.2–2 km the data records show irregularly spaced regions of strong gradients separated by sections with weak gradients, but otherwise lack conspicuous features. The general impression is one of strong stratification and only very weak levels of turbulence. Spectra of the gradient records from the upper kilometer exhibit distinct changes in slope at about 10^{-2} cycle per meter (cpm) and at 10 cpm. These changes in slope are interpreted as the scales at which different types of features dominate the vertical temperature profile: the nearly exponential mean profile is the principal feature for $K<10^{-2}$ cpm, while for $10^{-2}<K<2$ cpm the irregularly spaced structures in the stratification are the principal contributors to the spectra. Wavenumbers >10 cpm have been identified as the microstructure range and are characterized by a gradient spectrum which rises with increasing wavenumber until diffusion cuts off the temperature fluctuations. The levels of vertical microstructure activity are much lower than found at similar depths in the California Current, and unlike nearshore waters, little horizontal microstructure is found for scales <10 cm. Estimates of the vertical temperature diffusion coefficient K_Z from these records are much lower than those predicted by the diffusive thermocline models. However, the data are as yet too limited to regard this as a general conclusion for the central gyre region.

1. Introduction

During leg IX of the *Aries* cruise, September–October, 1971, vertical profiles of salinity and temperature were taken in the central North Pacific. For a period of two weeks, while the ship remained in the vicinity of 27N, 155W, the upper kilometer was sampled to a resolution of several meters by a commercial Salinity-Temperature-Depth recorder (STD). Free-fall microstructure recorder (MSR) drops, with a minimum resolution of a few centimeters, were made to depths ranging from 200 m to 2 km. Each MSR recording sampled a vertical column of approximately 150 m. Winds at shipboard level during the observations were light and steady at about 4 m sec^{-1}.

Our observation site is well into the Northern Subtropical Gyre and is typical of the regions modeled by the various thermocline theories in attempts to determine which of the possible convective and diffusive heat balances are important in producing the observed temperature profiles. As pointed out by Veronis (1969), the observed mean temperature gradient can be fitted equally well by thermocline models which assume that vertical diffusive processes balance the convective heat transport (e.g., Blandford, 1965), and by those which do not invoke vertical diffusion (e.g., Welander, 1959). Using scale depths similar to that of the thermocline shown in Fig. 1, the diffusive theories generally obtain values for K_Z, the coefficient of vertical diffusion, on the order of 10^{-4} m^2 sec^{-1}. Munk (1966) obtains a similar value from a model of the abyssal waters between 1 and 4 km.

By resolving the smallest scale of temperature fluctuations, vertical microstructure measurements can provide an independent estimate of the levels of vertical diffusion. A qualitative picture of the mixing is obtained by examining the records visually and attempting to identify specific processes by their characteristic signatures. Observations made near shore in the California Current by Gregg and Cox (1972), henceforth referred to as GC, found evidence for double diffusivity transport on the upper boundary of numerous temperature inversions as well as occasional meter scale overturns of the water. A more quantitative measure of the microstructure can be obtained from the spectra of the gradient records and from the total variance obtained from the spectra. Osborn and Cox (1972) showed that the ratio of the temperature gradient variance to the square of the mean gradient is related to the actual rate of vertical diffusion of heat compared to that which would occur due to diffusion along the mean gradients. To obtain an estimate of K_Z from this ratio it is necessary to make several assumptions. The strongest of these are 1) that the statistics of an oceanic region are known well enough to yield an average value of the temperature gradient variance, and 2) that there is no net lateral transport of temperature fluctuations into the region. If these are true, as well as several less

[1] Present affiliation: Department of Earth and Planetary Sciences, The Johns Hopkins University.

important assumptions, then

$$K_Z = k\frac{\overline{(\nabla\theta')^2}}{(\nabla\bar{\theta})^2},$$

where $\theta(Z)=\bar{\theta}(Z)+\theta'(Z)$, and k is the molecular coefficient of heat diffusion. In other sections of this paper we shall discuss the validity of these assumptions in the present work and in comparison with the near-shore results of Hacker *et al.* (1973), henceforth referred to as HCG.

In this paper we shall analyze both the STD and MSR data from the mid-Pacific and compare the results with our earlier work in the California Current.

2. Description of the data records

The STD data analyzed consisted of 13 records from the surface to 1 km. The FM signals from the instrument were digitized to produce several data points per meter and then interpolated to 1 m averages. Subsequent comparison with the accompanying Nansen bottles revealed that the temperature values were within the stated accuracy of the STD values, but some of the salinity records showed an offset which appeared to vary smoothly as a function of depth. For the data shown in Fig. 1 this was corrected by a least-squares fit of the STD record to the 12 salinities obtained from Nansen bottles taken at the same time. For comparison with the low wavenumber portion of the MSR observations, gradient records were computed by taking first differences of the STD values. Due to a malfunction in the salinity circuit excessive spikes were present in the salinity gradient records and they will not be considered.

Six MSR records have been analyzed, five of which were obtained in the upper 1 km and one from slightly deeper than 2 km. The instrumentation and data analysis are similar to those described by GC and HGC. In summary, the MSR records signals from two temperature sensors, a conductivity probe, and a vibrotron pressure gauge. Both 0.5-mm diameter glass-coated probe thermistors and 0.07-mm thick flake thermistors were used for the temperature measurements. One thermistor was mounted on the conductivity probe, suspended below the MSR, and the other on the tip of one of the rotating wing blades. Since the response time of the thermistors is influenced by the thickness of the boundary layer formed in the water around the probe, the response time is velocity-dependent. During these drops the MSR fell at 0.08 m sec^{-1}, and the tips of the wing blades travelled at 0.75 m sec^{-1} as they described a helical path during the descent. The power transfer function of the glass-coated thermistors was found to be best described by the function $L^2(\omega)=[1+(\omega\tau)^2]^{-2}$, where $\tau=0.022$ sec for the wing and 0.035 sec for the nose. Consequently, the power responses of the probes are attenuated by 6 db at a vertical scale of 0.02 m for the nose and at a scale of 0.16 m

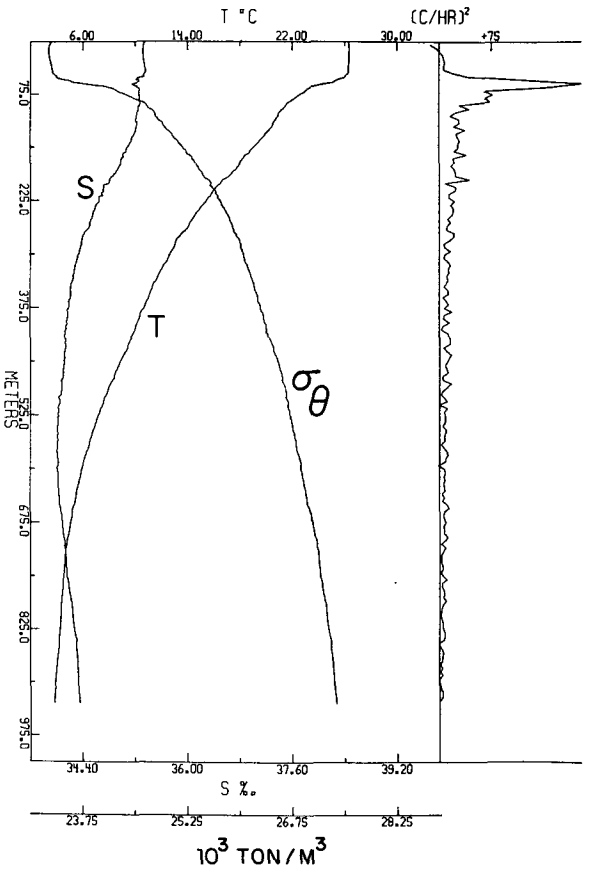

FIG. 1. Typical STD data obtained on the *Aries* IX cruise in the vicinity of 27N, 155W. Temperature (T), salinity (S), and potential density (σ_θ) are plotted at 1 m intervals. The square of the Väisälä frequency, computed from S, T and P averaged over successive 5 m intervals, is shown on the far right.

along the nearly horizontal wing path. Although a transfer function has not yet been obtained for the flake thermistors, preliminary tests show that they are at least as fast as the glass-coated probes. Since data obtained with the flakes has been corrected using the transfer function of the glass-coated thermistors, these results may be overcorrected at the highest wavenumbers. Due to the very low levels of microstructure activity in these records this will not affect the interpretation of the data.

The signals from the conductivity probe and the nose thermistor are each filtered to produce two separate records. One is produced by a high-pass, high-gain circuit and is interpreted as the vertical component of the conductivity, or temperature, gradient while the other results from a low-gain circuit and is recorded directly as gross conductivity or gross temperature. In order to compute the temperature from the gross temperature record it is necessary to know the water temperature at the beginning of the record. Due to the large temperature difference between the surface and the depth at which the data were taken, greater drift was experienced in the recorded signals than in our

previous work in the California Current. The resultant uncertainty in the depth at which the recording cycle started is estimated as ±30 m. Since there were no prominent features on the STD traces, it was not possible to determine the depth or initial temperature more precisely by comparing the gross temperature record with the STD. As a result of this uncertainty, only one of the salinity computations from the MSR records yielded good agreement with the mean salinity gradient.

3. Features in the vertical profiles

In comparison with records made near shore, these data are remarkable for the lack of identifiable features. As shown in Fig. 1, on scales greater than several meters, the temperature and salinity traces from the STD are very smooth, with temperature decreasing in a nearly exponential manner below the surface mixed layer. There was no suggestion of the sharp temperature and salinity changes which characterize the California Current at depths of several hundred meters. The temperature and salinity gradients below the mixed layer and above the salinity minimum at 600 m are in the proper sense for salt fingering to occur; at these depths the relative stability ratio, $\alpha\Delta T/(\beta\Delta S)$, varies between 3 and 4, where $-\alpha$ is the proportionate change in density due to temperature, and β is that due to salinity.

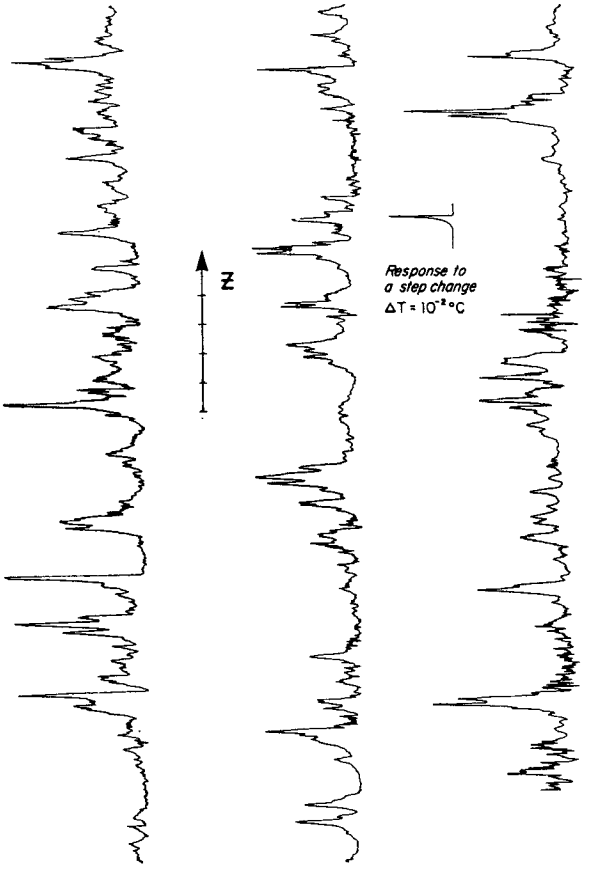

FIG. 2. Uncorrected temperature gradient record MSR 1. The plot begins at 215 m in the upper left hand corner and ends at 400 m at the lower right. The total length of the arrow represents 10 m in depth, Z positive upward. Only one data point out of 15 has been plotted, giving an appearance of higher microstructure levels than are present. A simple gradient scale cannot be given because the record has not been corrected for the transfer function of the high-pass filter. The response of the circuit to a step change of -10^{-2}C is shown as the calibration pulse.

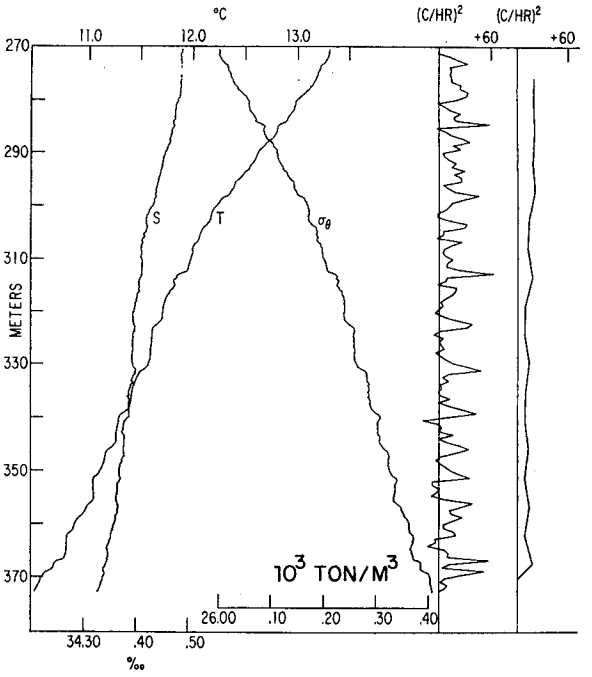

FIG. 3. Gross temperature, salinity and potential density for record MSR 4, plotted at 0.075 m intervals. The square of the Väisälä frequency shown on the far right was computed from S, T and P averaged over successive 3 m intervals, while the trace to the left used 0.68 m averages.

As seen in Fig. 2, the MSR records are also notable for the low levels of microstructure activity compared to the nearshore data. It should be noted that only every 15th data point has been plotted and the shortened aspect of the plot suggests higher levels of microstructure than are present. Although this profile has not been corrected for the transfer function of the high-pass filter or for the thermistor response, these corrections will have a noticeable effect only for structures <0.2 m. The only striking features are the narrow regions of strong gradients separating the more extensive intervals with weak gradients. In spite of the fact that the zero gradient has not been determined for this plot, it is obvious that there are no prominent temperature inversions, and no indication of even a meter scale instability of the type seen in the San Diego Trough.

No regularity in the spacing of the high-gradient regions is evident from Fig. 2. However, a 50 m deep section of one record, MSR 4, does exhibit a noticeable regularity. Fig. 3 shows the gross temperature and salinity for this record. The step-like structures begin-

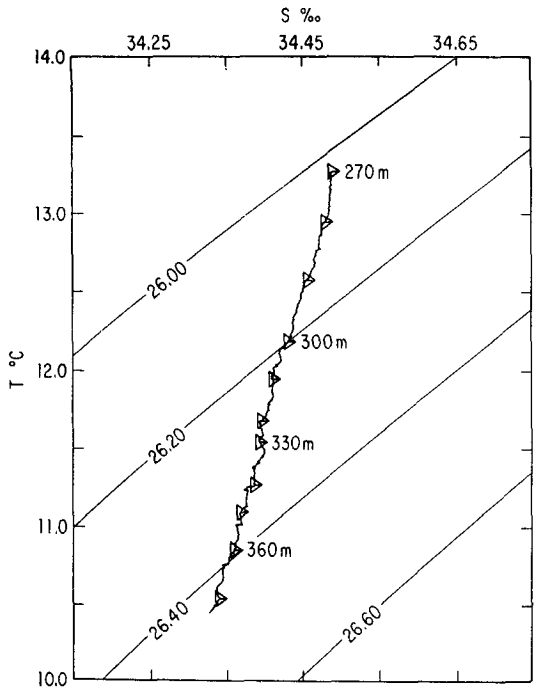

FIG. 4. T, S diagram for the data shown in Fig. 3. Contours are lines of constant σ_t.

ning slightly below 310 m are most evident on the plot of potential density. The T, S relation, as seen in Fig. 4, is quite linear at these depths, unlike the situation in the California Current. The characteristics of these structures have been estimated visually and are given in Table 1.

Although the salinity is generally decreasing with depth in this region, some of the high-gradient regions showed a net increase in salinity with depth. If true, salt fingering would not be possible at those sites. However, these salinity changes are quite small and may be due to the previously mentioned difficulties in the salinity calculation. The temperature gradient records for the nose and wing through this step-like region are shown in Fig. 5. The wing plot has been offset in the vertical direction so that it shows the same features as the nose at the same position on the plot. Both records have been scaled with the same time increment on the ordinate. Therefore, the arrow on the nose plot represents a vertical distance of 10 m while the corresponding arrow on the wing plot indicates a distance of 100 m along the helical path. In spite of the low angle of attack of the wing thermistor, about 6°, very little additional structure is seen, indicating that the fluctuations shown are indeed horizontal, with little suggestion of three-dimensional structures. The existence of salt fingers is not excluded, however, since 0.01 m thick temperature fluctuations would be well beyond the cutoff of the wing probe and could be missed by the nose if they are aligned vertically.

The only other identifiable feature from the MSR profiles is a 1 m thick temperature inversion at a depth of 915 m, seen in Fig. 6. This is the only temperature inversion of size greater than a few centimeters in these records. The integral of the gradient shows an S-shaped profile, suggestive of an overturn in an early stage. However, the levels of microstructure activity are much lower than those associated with similar features observed in the San Diego Trough, even when normalized by the mean gradient. If this is due to an overturn, its mixing effectiveness is rather low.

TABLE 1. Characteristics of gradient features in record MSR 4.

Mean thickness of high-gradient region	2.1 m
Mean thickness of low-gradient region	4.7 m
Mean ΔT across high-gradient region	0.075C
Mean ΔT across low-gradient region	0.039C

4. Calculation of the spectra

The spectra of the vertical temperature gradients have been patched together from three separate, but overlapping, spectra: the STD records which extend from 2×10^{-3} to 2×10^{-1} cpm, the gross temperature data from 1×10^{-2} to 6 cpm, and the high-gain nose

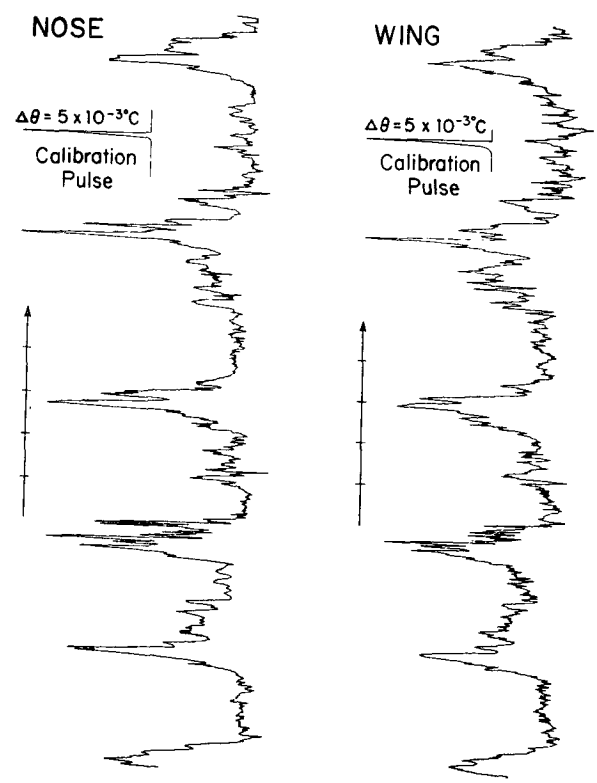

FIG. 5. Nose and wing temperature gradients for the step-like structures between 320–379 m in record MSR 4. The full length of the arrows represents 10 m and 100 m along the travel paths of the nose and wing, respectively. Equal time steps have been used for both records. The wing has been offset vertically so the same features can be compared.

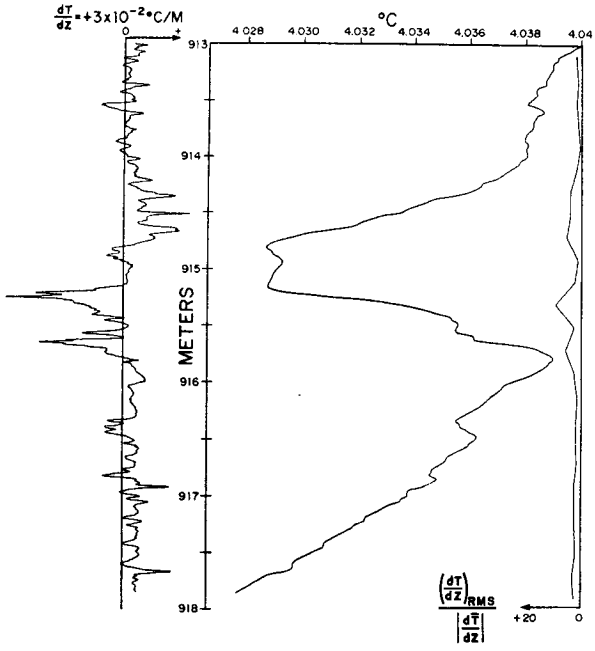

FIG. 6. S-shaped feature in the vertical temperature profile from record MSR 9. On the gradient scale Z is taken as positive upward; consequently, a positive gradient represents water which is becoming colder with increasing depth.

gradients from 1×10^{-1} to 6×10^{1} cpm. Let us first discuss the high-wavenumber spectra.

Since a record of 4096 words was found to provide the optimum spectral length, considering the computation time and the end effects associated with a finite record, the 80,000 word gradient record was broken into sequential 4096 blocks, which were prewhitened by taking first differences before the spectra were computed. The resulting spectra were corrected for the prewhitening, the transfer function of the MSR electronics, and the response of the thermistor. Each spectrum was averaged geometrically, i.e., the number of elementary bands per spectral point goes as 1, 2, 4, ... to a maximum of 64 elementary wavenumber bands per point and the final spectrum is formed by averaging across the 18 separate spectra. Therefore, the number of degrees of freedom varies with wavenumber from a minimum of 36 to a maximum of 2304. Because of the extreme variability of the spectral intensities the 95% confidence limits are worse than would be calculated for a Gaussian process, *viz.* (0.67–1.6) to (0.95–1.05).

When the electrical noise in the high-pass circuits is interpreted as temperature gradient, it follows a sharply rising curve at high wavenumbers. All of the spectral plots have been cut off where they become significantly affected by this noise. The effect of the correction for thermistor response can be seen in Fig. 12, which shows both the corrected and uncorrected spectral values. An error of $\pm10\%$ in the value of the nose thermistor response τ would produce errors of about $\pm30\%$ in the spectral estimate at $K=1\times10^{2}$ cpm.

The gross temperature data were averaged over 45 successive points, corresponding to 0.08 m in the vertical, and then first differences were taken, as was done with the STD data, to form gradient records containing the low-wavenumber information. Since geometrical averaging to a maximum of 32 elementary wavenumber bands was also performed on these spectra, the small number of degrees of freedom leads to a large statistical uncertainty. Thirteen of the STD spectra were ensemble-averaged resulting in 95% confidence limits of 0.63–1.87 at the lowest wavenumber and 0.92–1.09 at the points with maximum averaging.

5. Slopes of the spectra

Figs. 7 and 8 show the spectra of the temperature gradients from the *Aries* cruise. The STD sections, 100–612 m and 478–990 m, exhibit two regions with rather uniform slope: a rapid fall-off for $K<10^{-2}$ cpm and a very slow fall-off for $K>10^{-2}$ cpm. To determine whether the break in slope is due to the method of forming the gradient record from the original STD data, a separate calculation was performed in which the gradient record was prewhitened by taking second differences and then the resultant spectrum corrected for the prewhitening. Although a difference was observed for an individual spectrum, no significant variation due to the prewhitening occurred in the ensemble averages.

Three of the spectra of the gross temperature records show a maximum at about 0.1 cpm. Although MSR 4

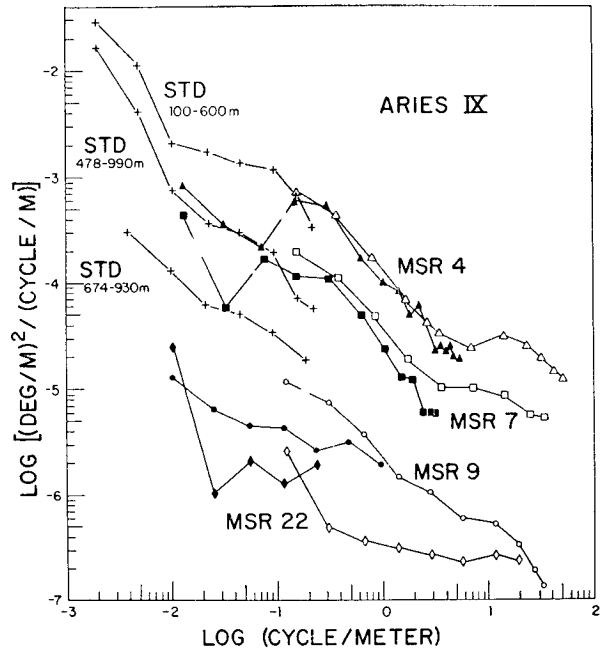

FIG. 7. Spectra of the vertical temperature gradients: ensemble averages of STD spectra (plus marks), MSR gross temperature (solid symbols), nose high-gain circuit (open symbols). Depths for MSR records are in Table 2.

shows a series of regularly spaced gradient features which could account for such a maximum, the confidence limits on the spectra at these wavenumbers are such that it is not statistically significant. The four shallower MSR records fall off with a nearly -1 slope for $K>0.6$ cpm, with an inflection in slope at 10 cpm. MSR 4 has a statistically significant maximum at $K=15$ cpm, and then a fall-off with a slope which is slightly less than -1. MSR 9 shows only a very weak inflection at high wavenumbers, and is then cut off sharply before it is noise dominated. The deep record, MSR 22, may be noisy at lower wavenumbers and is included for comparison with the more active record of MSR 9.

From the data plots previously discussed, we have observed three types of features in the temperature profile: the nearly exponential mean gradient, 1–2 m thick regions of strong temperature gradients which are irregularly spaced in depth, and centimeter-scale random temperature fluctuations which occur in varying intensity throughout the record. As shown in Fig. 9, we interpret the spectra of the records to be the composites of three different spectral signatures, each dominant in a different wavenumber range, representing three types of features. The rapid fall-off for $K<10^{-2}$ cpm is virtually the same for the ensemble average of the 13 individual STD spectra and for the spectrum of the average, as shown in Fig. 10. It is the signature of the nearly exponential mean profile and is the only feature common to the temperature records below the mixed layer.

For $K>10^{-2}$ cpm the transient gradient features are more intense than the mean gradient; although, as seen in Fig. 10, the weakening of the main thermocline with increasing depth results in a less distinct break in slope than at shallower depths. This spectral domain reflects the irregularly spaced strong gradients separated by regions with weak gradients. The rather flat spectrum of the temperature gradient in this wavenumber band corresponds to a -2 slope in the temperature spectrum, the form associated with "stepped" structure

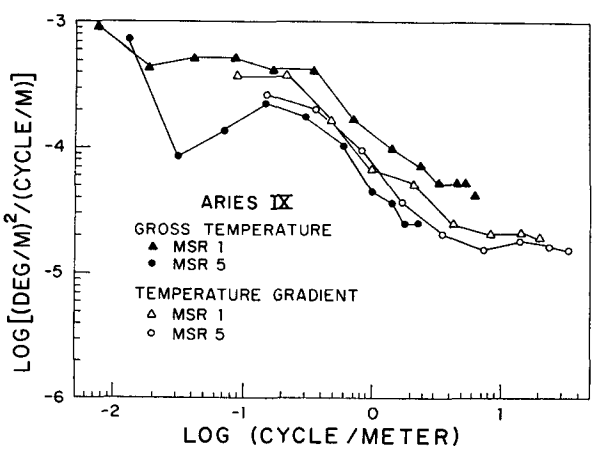

FIG. 8. Spectra of MSR temperature records.

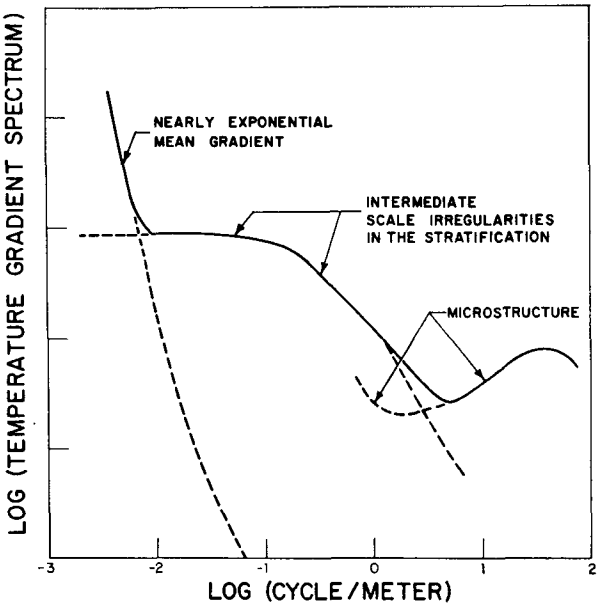

FIG. 9. Schematic spectra of the vertical temperature gradients in the main thermocline. The solid lines represent the sum of the three components shown by dotted lines.

in the profile (Phillips, 1971). The spectral roll-off begins about 0.2 cpm. From the data plots in Figs. 2 and 5 this is the scale at which we would expect the thickness of the gradient structures to begin to influence the spectra.

The change in slope at about 10 cpm is weak in the mid-gyre spectra, but nevertheless statistically significant. As shown by HCG, all of our measurements from the San Diego Trough show an inflection in slope followed by a very distinct maximum. Such a maximum could be the result of a turbulent velocity structure producing nearly isotropic temperature fluctuations at high wavenumbers or of a preferred vertical spacing between thin horizontal structures. In the Trough most of the contribution to this maximum has been found to come from a few 1 m scale regions in the vertical profile.

To consider the microstructure region more fully, Fig. 11 shows a schematic spectrum of the vertical temperature gradients which might be expected for a patch of strong turbulence in an otherwise smoothly stratified fluid. If L is the vertical dimension of the patch, then K_L [cpm]$=1/L$ is the scale at which the gradient spectrum should begin to increase in intensity with increasing wavenumber. For $K<K_L$ the stratification results in a falling spectrum. The other wavenumbers shown in Fig. 11 may be identified as follows: K_B is the scale of the largest eddies which can be isotropic, K_V the scale at which viscosity smoothes the velocity fluctuations, and K_T the scale where diffusion cuts off the temperature irregularities. For $K_L<K<K_B$ the vertical turbulent motions should be strongly affected by the stratification and will be anisotropic in nature. Several authors (Bolgiano, 1962; Lumley, 1964;

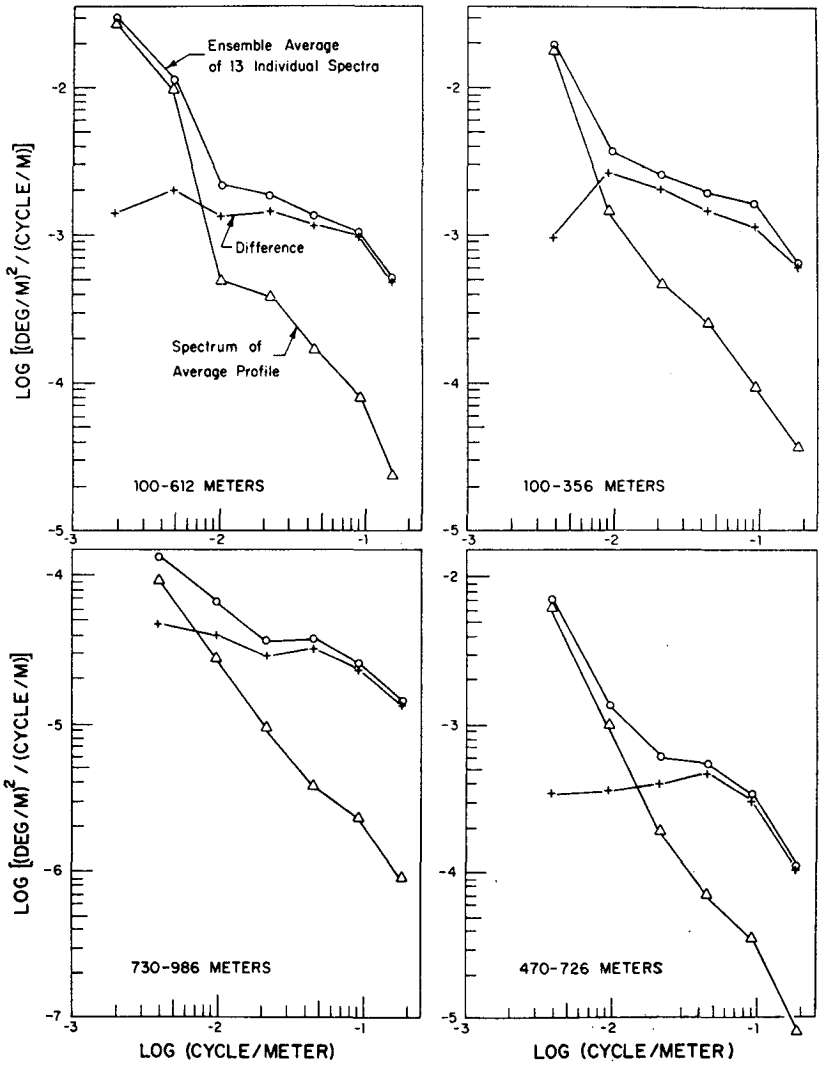

FIG. 10. Comparison of ensemble average of STD spectra with spectrum of the average.

Lin *et al.*, 1969) have argued for the existence of a distinct buoyancy subrange for this situation and have proposed a variety of slopes for the three-dimensional spectrum. We find no evidence for such a distinctive subrange in our data and show this region as a transition from the scale at which the ocean is completely stratified to the smaller scales which are possibly approaching isotropy.

The table in Fig. 11 evaluates the wavenumber scales for values of the Väisälä frequency found in mid-gyre and for values of the energy dissipation which bracket those expected, below the near surface layers of the ocean, from the mean rates of energy input due to tides and winds. As the energy dissipation decreases, the separation of the wavenumber scales K_B, K_V, K_T also decreases until for 10^{-10} m^2 sec^{-3} we have K_V and K_T less than or approximately equal to K_B. Thus, for such weak levels of turbulence there will not be a sequence of subranges in the high-wavenumber spectra, but only a short dissipation range in which the spectral levels increase to the scale at which diffusion smoothes the temperature fluctuations.

Since our spectra in Figs. 7 and 8 represent the average spectral levels over a 150 m column, the rising contribution to the spectrum with increasing wavenumber due to a patch of strong turbulence will be superimposed upon a falling spectrum which reflects the stratification in other parts of the record. Our own previous work as well as the towed measurements of Nasmyth (1970) and the visual observations of Woods (1968) have so far failed to find any turbulent patches with a vertical extent greater than about 2 m. Accordingly, for a patch of strong turbulence K_L should be in the range $0.5 < K_L < 2$ cpm. Since this is in the same range as the stable regions of high-temperature gradient, the composite spectrum will not necessarily have a minimum which is directly related to K_L, the scale of the overturning region. Rather, a minimum will occur

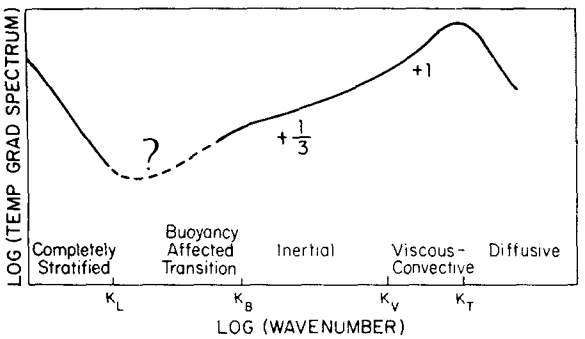

ϵ (M²/SEC³)	$K_B=\frac{1}{2\pi}\left(\frac{N^3}{\epsilon}\right)^{1/2}$ (CYCLE/M)	$K_V=\frac{1}{2\pi}\left(\frac{\epsilon}{\nu^3}\right)^{1/4}$ (CYCLE/M)	$K_T=\frac{1}{2\pi}\left(\frac{\epsilon}{\nu K^2}\right)^{1/4}$ (CYCLE/M)
10^{-7}	.25-.10	74	225
10^{-8}	.80-.33	41	127
10^{-9}	2.5-1.0	23	71
10^{-10}	8.0-3.3	13	40

N = 3.6-2 CYCLE/HOUR

FIG. 11. Form of the vertical temperature gradient spectrum expected for a patch of fully developed turbulence in an otherwise stratified fluid. K_L represents the wavenumber scale of the energy containing eddies, K_B the maximum scale for which eddies can be isotropic, K_V the viscous cutoff of velocity fluctuations, and K_T the diffusive cutoff of temperature variations. The scales are estimated for ranges of the energy dissipation ϵ, which bracket those expected in the ocean.

where the rising microstructure spectrum intersects the falling curve representing the structure of the stratification. For higher microstructure levels this intersection will occur at lower wavenumbers. In view of the strong stratification and weak levels of turbulence shown by our data plots from mid-ocean and since the wavenumber scales in Fig. 11 were derived on the assumption of strong turbulence, it is not possible to directly apply that scaling to infer the energy dissipation.

6. Comparison with the San Diego Trough

In Fig. 12, spectra of the most active of the mid-Pacific data are compared with a moderately active record from the San Diego Trough. This nearshore record is the same one in which GC found several patches of strong microstructure activity including a meter scale instability in the density profile. *Aries* MSR 4 has, however, only slightly lower spectral levels than the least active record which HCG reported for the Trough. Although the mean temperature gradient for the *Aries* record is twice that for the one near shore, its spectrum is a factor of 50 lower in the microstructure range, and at least a factor of 2 lower elsewhere. In addition to the higher spectral levels, the slopes of the Trough spectra also suggest stronger levels of turbulence; the spectral minimum, where the rising microstructure spectrum intersects the falling stratification

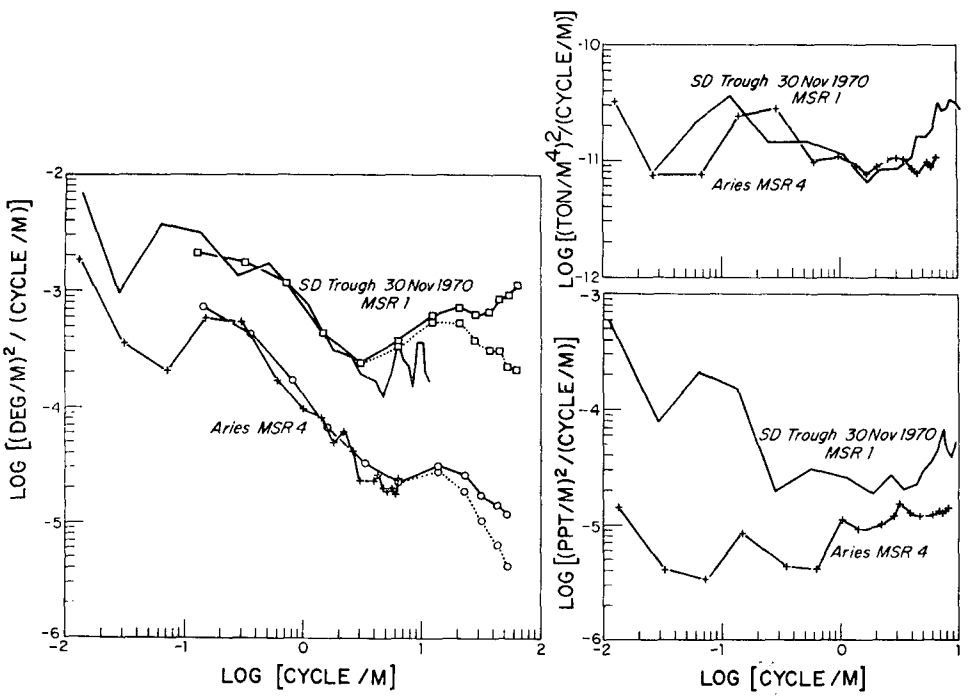

FIG. 12. Comparison of the highest spectral levels from the mid-ocean data, MSR 4, with moderate levels from the San Diego Trough. The salinity and temperature spectra are of the gross records only. The high-gain nose temperature gradient records are shown by the open symbols. The dotted lines at high wavenumber show the gradient records which have been corrected for the transfer function of the circuit but not for attenuation of the thermistor. The solid line includes this correction.

spectrum, occurs at a lower wavenumber and the dissipation maximum occurs at higher wavenumbers.

For wavenumbers near 1 cpm, a -1 slope in the Trough gradient spectrum parallels the similar feature in the *Aries* data. Similar regions of roughly -1 slope occur in all of our spectra, generally in the wavenumber range $0.6<K<6$ cpm. As previously mentioned, we consider this to be a feature of the stratification rather than of any turbulent structures present. If this were considered to be due to a buoyant subrange, the salinity spectrum would be expected to show the same slope, and this is not the case in either record. Although the Trough temperature and salinity spectra are considerably higher than those of MSR 4 in this wavenumber range, the spectra of the potential density gradients are nearly the same in level and slope. These salinity spectra have been computed from the gross records and may be affected by noise for wavenumbers close to 10 cpm.

The relative contributions of different wavenumbers to the temperature gradient variances are also different between the nearshore and mid-ocean data. In Fig. 13

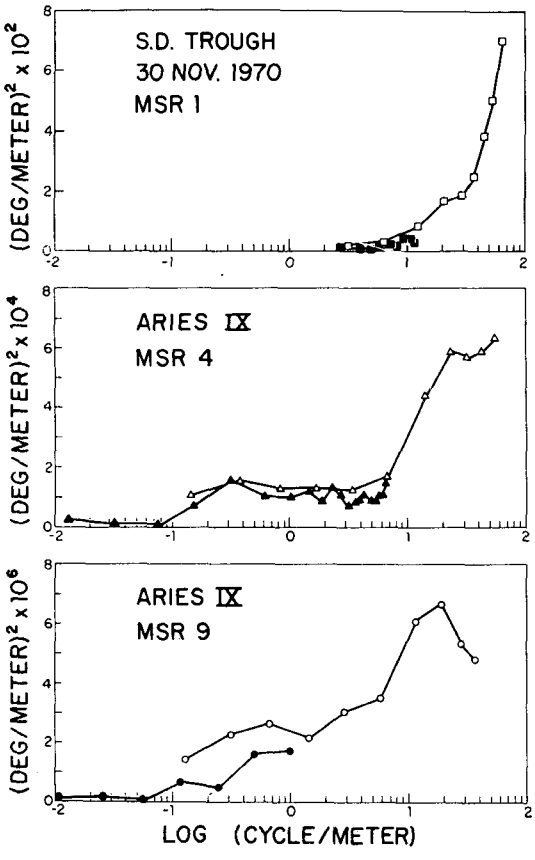

FIG. 13. The product of the wavenumber and the spectral level on a linear ordinate versus wavenumber on a logarithmic scale. Thus, equal areas under the curves represent equal contributions to the temperature gradient variance. Closed symbols represent the differentiated gross temperature record and open symbols show the high-gain gradient data.

TABLE 2. Contributions to the temperature gradient variance by wavenumber decades. The contribution for $k>0.1$ cpm extends to the noise limit of the signals.

RECORD	DEPTH	$\left(\frac{d\bar{T}}{dz}\right)^2$	Contributions to Temp. Gradient Variance by Wavenumber Decades (CYCLE/METER) 10^{-2}-10^{-1}	10^{-1}-10^{0}	10^{0}-10^{1}	$>10^{1}$	$\overline{(dT/dz)^2}$	$\frac{\overline{(dT/dz)^2}}{(d\bar{T}/dz)^2}$
ARIES IX	METERS	$(°C/m)^2$	$(°C/m)^2$	$(°C/m)^2$	$(°C/m)^2$	$(°C/m)^2$	$(°C/m)^2$	
MSR 1	215-400	7.8×10^{-4}	6.2×10^{-5}	2.2×10^{-4}	3.1×10^{-4}	4.2×10^{-4}	1.0×10^{-3}	1.3
MSR 4	270-373	6.9×10^{-4}	4.4×10^{-5}	2.4×10^{-4}	2.7×10^{-4}	9.5×10^{-4}	1.5×10^{-3}	2.2
MSR 5	300-410	5.3×10^{-4}	1.9×10^{-5}	1.1×10^{-4}	1.7×10^{-4}	4.0×10^{-4}	7.0×10^{-4}	1.3
MSR 7	550-672	1.5×10^{-4}	1.7×10^{-5}	6.2×10^{-5}	1.0×10^{-4}	1.2×10^{-4}	3.0×10^{-4}	2.0
MSR 9	900-1056	1.1×10^{-5}	4.0×10^{-7}	3.3×10^{-6}	6.0×10^{-6}	9.4×10^{-6}	1.9×10^{-5}	1.7
MSR 22	2000-2153	6.6×10^{-6}	3.8×10^{-7}	3.2×10^{-6}	1.8×10^{-6}	4.0×10^{-6}	9.4×10^{-6}	1.4
SD Trough 30 Nov 70 MSR 1	212-340	1.8×10^{-4}	4.6×10^{-4}	1.2×10^{-3}	2.7×10^{-3}	4.7×10^{-2}	$>5.1\times10^{-2}$	>286

the product of the wavenumber and the spectral level are plotted on a linear ordinate scale against a logarithmic abscissa. Since equal areas under the curves represent equal contributions to the temperature gradient variance, it is seen that *Aries* MSR 9 is the only record which clearly has been resolved to show decreasing contributions to the temperature gradient variance with increasing wavenumber. The degree to which we have resolved the more active records is as yet uncertain.

Although the *Aries* spectra show an appreciable contribution to the temperature gradient variance for wavelengths as low as 0.1 cpm, the Trough records have negligible variance contributed from scales less than 6 cpm. The contributions to the variance by decades of wavenumber are shown in Table 2, as well as the ratios of the mean square gradients to the squares of the mean gradients. Although the variance of the *Aries* data varies by a factor of 100 from the shallower to the deep records, the ratio of the variances to the squares of the mean gradients shows a range of less than 2. Thus, over the upper 2 km the normalized microstructure levels are uniformly low, showing little depth dependence.

If we assume that the contribution of the lateral terms to the net entropy generation is negligible, then the Osborn and Cox model yields a vertical temperature diffusion coefficient,

$$K_Z = 2k = 2.6\times10^{-7}\ \text{m}^2\ \text{sec}^{-1},$$

for the *Aries* records and 3.7×10^{-5} m^2 sec^{-1} for the San Diego Trough. The mid-gyre values are thus a factor of 400 below those estimated by the diffusive thermocline theories. During the observation period in mid-gyre, measurements made over a 20-mi radius failed to show any features, below the mixed layer, which could be traced laterally from the STD records. This fact in connection with the uniform levels of the normalized microstructure suggest that the data form a representative average, for this particular location

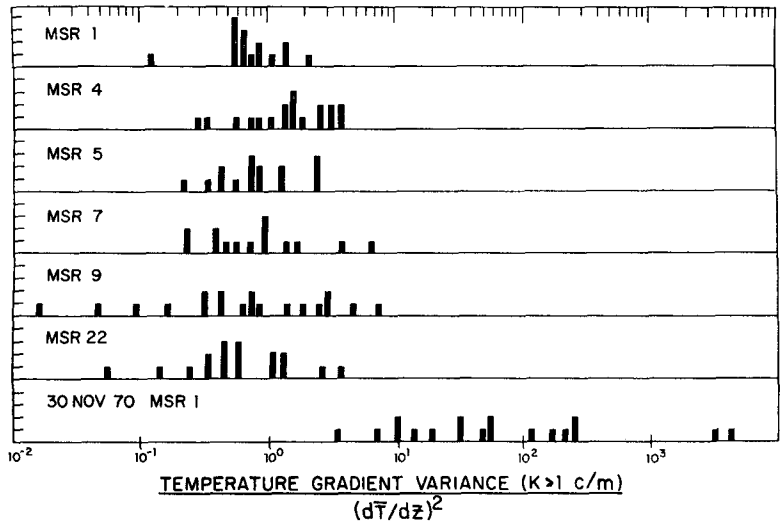

FIG. 14. Histograms of normalized variances for individual 4096 point spectra.

and time, and that the lateral terms are minimal. The data in the San Diego Trough, however, show a great scatter between successive measurements and there is marked lateral inhomogeneity. Therefore, the application of the Osborn-Cox model seems warranted for the *Aries* measurements, but more data will be required in the California Current to obtain representative averages and evaluate the lateral effects.

The temperature gradient variance, normalized by the square of the mean gradient for each drop, definitely does not follow a normal distribution. For each of the individual 4096 word blocks used in computing the spectra the contributions to the variance for wavenumbers >1 cpm were computed and then normalized by the square of the mean gradient of the complete data record. In Fig. 14 are shown histograms of the distribution of the logarithms of these normalized variances. Although the shallower *Aries* drops show a range of slightly more than one decade and the deeper ones two decades, the *Aries* data are clearly a different population from those of the Trough. The nearshore profile has a span of three decades in the variance and a median value 50 times greater than the *Aries* records. The outlying values for the deep *Aries* drops represent very low microstructure values, while the two extreme variances in the Trough are due to a meter scale overturn and double diffusivity steps. As shown in Fig. 15, all of the *Aries* data taken together give a moderate fit to a straight line on a logarithmic probability plot, although the observed data have a higher probability at both ends of the range than a log-normal distribution. Since the chi-square test gives a probability of only slightly greater than 10% that the observed deviation of the logarithms could be due to chance alone, the distribution must be regarded as approximately log-normal. Several investigators (Obukhoff, 1962; Kolmogoroff, 1962; Yaglom, 1966; Mandelbrot, 1972) have argued that the effect of intermittency in otherwise homogeneous turbulence is to produce a distribution of the dissipation of energy and scalar variables which is at least approximately log-normal. Although our measurements definitely do not fit the assumptions in these derivations, the vertical temperature dissipation does seem to be roughly log-normal. We find this to be a curious result for which we have no explanation.

7. Three-dimensional structure

The relative spectral levels of the wing and nose confirm that the intensity of turbulent activity is con-

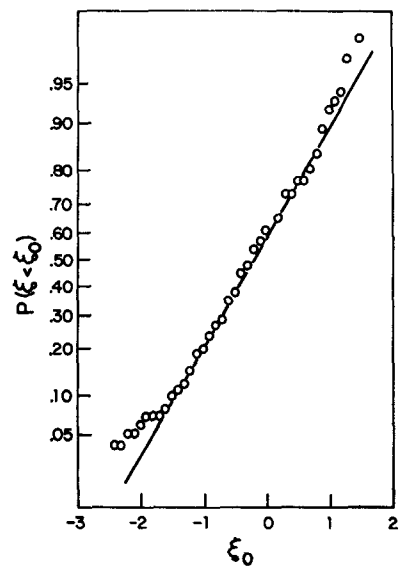

FIG. 15. Probability distributions of temperature gradient variance (for $K>1$ cpm) compared with log-normality. There are 96 samples composed of 4096 data points each.

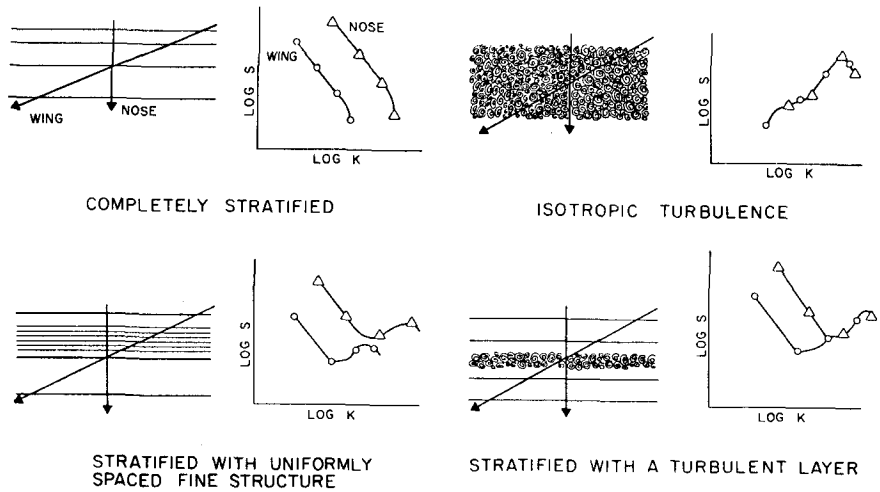

FIG. 16. Schematic high-wavenumber temperature gradient spectra for wing and nose probes assuming both sensors can resolve all structures present.

siderably lower than found by HCG in the Trough. This measurement technique is summarized in Fig. 16, which shows the relative spectral levels that would occur in different water structures. The wing record is interpreted as the temperature gradient along its helical path, which is inclined 6° to the horizontal. Consequently, the wing spectra extend to lower wavenumbers than those of the nose. As was pointed out by Frank Lane (private communication) the spectral level of the wing can approach that of the nose either as a consequence of an increase in horizontal layering with small vertical separations or as a result of isotropic temperature structures. If both probes could resolve the diffusive cutoff then it would be possible to determine whether the high-wavenumber spectral maximum is due to patches of isotropic structures as in Fig. 16d, or to an increase in the degree of layering at high wavenumbers, as in Fig. 16c.

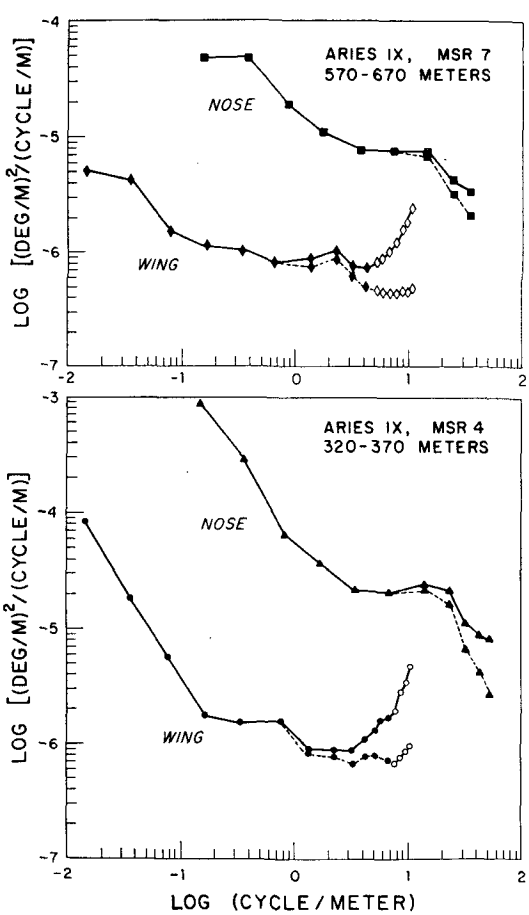

FIG. 17. Wing and nose spectra for two *Aries* records. Dotted lines show spectra without corrections for thermistor response. Open symbols show spectrum after it is dominated by noise.

Spectra of two matching nose and wing records are shown in Fig. 17. The spectra for MSR 4 were calculated for the data plotted in Fig. 5. Even including the noise contribution, shown by the open symbols, the corrected wing spectra are a factor of 4 below the nose spectra at $K=10$ cpm. This is in marked contrast to the situation in the San Diego Trough, where the corrected wing spectral estimates equaled those of the nose spectra in the range of 10–30 cpm, and even the uncorrected wing spectra rise to within a factor of 3 of the nose spectra at 5 cpm. Most of the structures contributing to the high wing spectra in the Trough came from the one overturning region and are presumably approaching isotropy. There is no such region in either MSR 4 or 7, and if there is an approach to isotropy it must occur at wavenumbers much greater than 10 cpm.

8. Summary and conclusions

These measurements from one locality in the central North Pacific in early autumn have shown temperature and salinity profiles which appear very smooth on vertical scales greater than several meters. STD stations

within a 30 km radius failed to find any features other than a mixed layer and a salinity minimum at 600 m, which is common to the North Pacific. This location thus exhibits the lateral homogeneity and nearly exponential profile described by the various thermocline models. High-resolution observations from free-fall vehicles also revealed a paucity of features, other than regions of sharp temperature gradients separated by sections with much weaker gradients. There was one 50 m interval in which the spacing of these features seemed regular, otherwise the spacing was irregular.

In summary, the presence of centimeter-scale temperature fluctuations, having a diffusive time scale of a few minutes, in these records implies that weak levels of turbulent stirring occur throughout the water column. From this set of measurements it does not seem possible to separate which of the meter-scale gradient features are due to internal waves and which are the boundaries between different water types. If some do represent structures in the water they have a maximum diffusive time scale of a few months and suggest that more vigorous stirring must have occurred prior to our observations.

Spectra of the vertical temperature gradients seem to show three regions, separated by breaks in slope, which are the consequence of different dynamical processes: 1) wavenumbers less than 10^{-2} cpm are dominated by the nearly exponential mean temperature gradient, whose spectrum exhibits a rapid fall-off with increasing wavenumber until, 2) for wavelengths greater than 10^{-2} and less than 5 cpm, the spectrum is dominated by the irregularly-spaced high-gradient regions. [This is the domain of the layering remarked upon by other observers, although we do not find it to be very regular.]; finally 3) in data which show moderate or high levels of microstructure, there is an inflection at about 5 cpm. This inflection takes the form of a minimum in spectral intensity, followed by a maximum at higher wavenumbers. The final fall-off of the spectra is the scale at which the fluctuations of temperatures are being dissipated by diffusion. Although the microstructure portion of the nearshore spectra is dominated by the contributions of a few small patches, in mid-gyre the microstructure activity is distributed much more uniformly along a 150 m long record. For the deep records, this microstructure range is virtually absent.

In spite of the fact that the mean temperature gradient in the data reported here is twice that in the San Diego Trough, the spectral levels are lower at all wavelengths, and by a factor of more than 50 in the microstructure range. Clearly, the velocity shears which generate the microstructure temperature gradients must be much weaker at the mid-ocean site. The Osborn-Cox model, which provides a way to estimate the vertical diffusion associated with the microstructure levels, indicates that the vertical diffusion is a factor of 400 below those levels expected from the diffusive thermocline theories. Although we did not quantitatively evaluate the assumption of lateral homogenity in this model, this site in mid-gyre seems to be as uniform and featureless as can be found. In view of the spectral levels and the appearance of the data it is difficult to escape the assumption that the vertical diffusion shown by these records is barely above that due to molecular conduction along the mean gradients. This is in marked contrast to the situation near shore.

This set of measurements is a very limited sample, both in time and space. It may be that the mean levels of vertical heat transport in mid-gyre are much higher than reported here and occur as vigorous, but occasional (or even seasonal), events which were missed by these observations.

Acknowledgments. This work has been supported by the Office of Naval Research and the Advanced Research Projects Agency. As usual, we are indebted to Bill Johnson and Jack Lucas for help with the instrumentation and collection of the data. Programming assistance was provided by Arne Mortensen and John Muryama. Helpful discussions were enjoyed with Frank Lane and Carl Gibson.

REFERENCES

Blandford, R., 1965: Notes on the theory of the thermocline. *J. Marine Res.*, **23**, 18–29.

Bolgiano, R., 1962: Structure of turbulence in stratified media. *J. Geophys. Res.*, **67**, 3015–3023.

Gregg, M., and C. Cox, 1972: The vertical microstructure of temperature and salinity. *Deep-Sea Res.*, **19**, 355–376.

Hacker, P., C. Cox and M. Gregg, 1973: Spectra of high-resolution temperature profiles in the San Diego Trough (in preparation).

Kolmogoroff, A. N., 1962: A refinement of previous hypotheses concerning the local structure of turbulence in a viscous incompressible fluid at high Reynolds number. *J. Fluid Mech.*, **13**, 82–85.

Lin, J. T., S. Panchev and J. E. Cermak, 1969: A modified hypothesis on turbulent spectra in the buoyancy subrange of stably stratified shear flow. *Radio Sci.*, **4**, 1333–1337.

Lumley, J. L., 1964: The spectrum of nearly inertial turbulence in a stably stratified fluid. *J. Atmos. Sci.*, **21**, 99–102.

Mandelbrot, B. B., 1972: Possible refinement of the log-normal hypothesis concerning the distribution of energy dissipation in intermittent turbulence. *Lecture Notes in Physics*, Vol. 12, *Statistical Models in Turbulence*, Berlin, Springer-Verlag.

Munk, W. H., 1966: Abyssal recipes. *Deep-Sea Res.*, **13**, 707–730.

Nasmyth, P. S., 1970: Ocean turbulence. Ph.D. thesis, University of British Columbia.

Obukhoff, A. M., 1962: Some specific features of atmospheric turbulence. *J. Fluid Mech.*, **13**, 77–81.

Osborn, T., and C. Cox, 1972: Oceanic fine structure. *Geophys Fluid Dyn.*, **3**, 321–345.

Phillips, O. M., 1971: On spectra measured in an undulating layered medium. *J. Phys. Oceanogr.*, **1**, 1–6.

Veronis, G., 1969: On theoretical models of the thermocline circulation. *Deep-Sea Res.*, **16**, Suppl., 301–323.

Welander, P., 1959: An advective model of the ocean thermocline. *Tellus*, **11**, 309–318.

Woods, J., 1968: CAT under water. *Weather*, **23**, 224–235.

Yaglom, A. M., 1966: The influence of the fluctuation in energy dissipation on the shape of turbulent characteristics in the inertial interval. *Sov. Phys. Dokl.*, **11**, 26–29.